Journal of Thermal Analysis and Calorimetry, Vol. 70 (2002) 173–179

THERMALLY ACTIVATED CRYSTALLIZATION OF TWO FeNiPSi ALLOYS

J. J. Suñol[1*], *M. T. Clavaguera-Mora*[2] *and N. Clavaguera*[3]

[1]Department of Physics, EPS (P II), Universitat de Girona, 17071 Girona, Spain
[2]Department of Physics, Facultat de Ciències, Universitat Autònoma de Barcelona, 08193 Bellaterra, Spain
[3]Department of ECM, Facultat de Física, Universitat de Barcelona, 08028 Barcelona, Spain

Abstract

The crystallization kinetics of two alloys in the Fe–Ni–P–Si quaternary system have been investigated, with both isothermal and continuous heating experiments, by means of differential scanning calorimetry. Both alloys present two separated crystallization processes. The Johnson–Mehl-Avrami–Erofeev equation with a rate constant following the Arrhenius behavior gives the best fit of the experimental data. In all processes the value of its JMAE kinetic exponent is not constant. In the nearly stages, n changes steeply revealing the transient nucleation effect to reach values corresponding to a three-dimensional volume growth controlled by diffusion in the central part ($0.3<x<0.55$). Latter in the transformation n continuously decreases reflecting the saturation of nucleation.

Keywords: crystallization, DSC, Fe–Ni alloys, melt-spinning

Introduction

The field of rapid solidification of metals and alloys from the liquid state has undergone enormous progress during the last decades. This started with the successful rapid quenching experiments of Falkenhagen and Hoffmann [1] and Duwez *et al*. [2, 3], where different extended solid solutions were obtained. A large number of metastable materials, such as amorphous phases, extended solid solutions and non-equilibrium crystalline phases, have been produced.

The Fe–Si based metallic glasses produced by melt spinning have been the object of much scientific and technological attention during the last twenty years [4, 5], particularly because of their soft magnetic properties which are usually better than those of conventional crystalline materials. Magnetic properties are influenced by the crystallization and the thermal behavior of metallic glasses has been studied extensively. One way to perform this analysis is the construction of the transformation diagrams temperature – time (T-T-T) and heating rate – time (T-HR-T) [6]. Furthermore, other fields were the kinetics of the metallic glass oxidation in air below the

* Author for correspondence: E-mail: joanjosep.sunyol@udg.es

1418–2874/2002/ $ 5.00
Akadémiai Kiadó, Budapest
© 2002 Akadémiai Kiadó, Budapest
Kluwer Academic Publishers, Dordrecht

glass transition temperature [7] or the modeling of the crystal to amorphous transition on the atomic scale [8]. Moreover, the crystallization kinetics of metallic glasses shows a wide spread of the activation energies. Recently, this spread in the literature was attributed to differences in the quenching rates and the presence of variable number of quenched-in nuclei [9–10].

In this paper we report on the crystallization behavior of a FeNiPSi rapid quenched glass alloy. The determination of the temperatures, activation energies and kinetic analysis of each stages of crystallization has been derived from differential scanning calorimetry (DSC) results. The amorphous state of the non-treated specimens was demonstrated by X-ray diffraction and transmission Mössbauer spectroscopy in previous works [11, 12].

Experimental

Sample preparation

In this work, the Fe–Ni based quaternary alloys were obtained by rapid solidification, i.e., melt spinning. The precursors used were pressed powders of elemental Fe, Ni, Si, P and Fe_3P (to prevent P sublimation). The quaternary alloys analyzed are chosen to be 80% metal–20% metalloid include both Si and P. The nominal compositions of the metallic glass ribbons studied are: $Fe_{40}Ni_{40}P_{20-x}Si_x$ with x=7 and 10, labeled as A and B respectively. Pure elements (<99.9 at%) and small particle sizes were chosen (smaller than 25 μm) as precursors. The working conditions of the device were chosen to obtain amorphous alloys. To reduce influences of the production conditions on the ribbons properties the same parameters were employed to obtain both alloys. The alloys were prepared by rapid quenching from melts which were treated at 1050°C during 10 min. The ribbons were produced, by quenching the molten alloy on the surface of a rapidly spinning (about 30 m s^{-1}) Cu wheel. The working atmosphere was inert, Ar. The ribbons were about 0.2 cm wide and 25 μm thick.

Methods

The calorimetric experiments were carried out in a DSC7 Perkin Elmer calorimeter under an inert argon atmosphere. The crucible material was aluminum and the amount of the samples was about 5 mg. Thermal stability was analyzed via isothermal and non-isothermal experiments. Isothermal measurements were performed at a heating rate of 300 K min^{-1} until the annealing temperature was reached. The temperatures of the isothermal sections were 670 and 725 K for alloy A and 685 and 735 K for alloy B, these isothermal temperatures were selected below the onset temperatures of the crystallization processes.

The experiments at constant heating rate were recorded from room temperature up to temperature, above the exothermal crystallization, at scan rates ranging from 5 to 80 K min^{-1}.

Kinetics analysis and discussion

This kind of alloys presents at least two separate stages of crystallization when heated [11, 12]. Usually the first process corresponds to the crystallization of the main crystalline phase and the second one to the crystallization of the amorphous remaining phase. In the two alloys analyzed in this study, both crystallization processes are well separated in temperature and can be studied individually in both isothermal and continuous heating conditions. The heat evolved in the first stage of crystallization is higher (81/78 J g^{-1} in alloys A/B) to that evolved in the second one (12/10 J g^{-1} in alloys A/B). The apparent activation energies, E, are obtained from Kissinger [13], Ozawa [14] and multiple scan methods [15]. As well known, these methods use logarithm linearization and not consider all data from DSC measurements. For that reason they are very sensitive to the experimental errors. Nevertheless, we use these methods in this work as a first approach to perform the kinetic analysis. The average values of the activation energies are given in Table 1.

Table 1 Apparent activation energy of the different crystallization processes

Crystallization process	Activation energy/kJ mol^{-1} ±20
A (process 1)	637
A (process 2)	463
B (process 1)	453
B (process 2)	405

To explain the thermal behavior of the glasses upon crystallization, we assume a rate of reaction given by

$$\frac{dx}{dt} = k(T) f(x) \tag{1}$$

where x is the crystallized fraction at time, t, and temperature, T, $k(T)$ is the rate constant and $f(x)$ is a function that reflects the mechanism of crystallization. These two functions are assumed to be independent of the thermal history of the sample, with an Arrhenius form of the rate constant, under both isothermal and continuous heating conditions. To check the validity of the method irrespective of the experimental procedure (isothermal or continuous heating) a usual graph method is the plot of $\ln(dx/dt)$ *vs*. $1/T$ [16].

Once the value of the apparent activation energy is known, the function $f(x)$ can be evaluated from the continuous heating and from isothermal experiments. If the kinetic behavior is the same in both kinds of experiments, the experimentally measured $\ln(k_0 f(x))$ *vs*. $\ln(1-x)$ has to be independent of heating rate and identical to that obtained in an isothermal regime. That expression can be evaluated from dx/dt by taking

$$\ln(k_0 f(x))=\ln\left(\frac{\mathrm{d}x}{\mathrm{d}t}\right)-\frac{E}{RT} \quad (2)$$

Furthermore, the analysis of the function $f(x)$ is useful if we want to distinguish which one of the several existing kinetic models can best describe the crystallization process. All measured DSC curves for every crystallization stage can be directly compared.

In order to perform the kinetic analysis and to decide which kinetic model agrees better with our experimental crystallization data as the crystallized fraction x. We compare the experimental dependence of $\ln(k_0 f(x))$ *vs.* $\ln(1–x)$ and that predicted, assuming different model equations for $f(x)$. This or other equivalent graphs were used by several authors [17–19].

The kinetic model that gives the best fit to our experimental data in the two stages of crystallization of both alloys can be unambiguously represented by the Johnson–Mehl–Avrami–Erofeev (JMAE) equation $f(x)=n(1–x)(–\ln(1–x))^{(n–1)/n}$ where n is the kinetic exponent. Figures 1 to 4 show the results obtained in the crystallization stages (labeled as 1/2 the low / higher temperature process) of both samples. No significant changes are detected as a function of P/Si ratio.

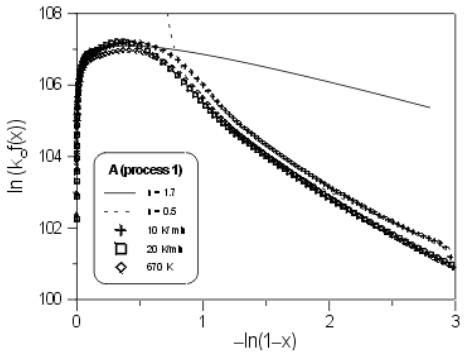

Fig. 1 Plot of $\ln(k_0 f(x))$ *vs*. $–\ln(1–x)$ for the low temperature crystallization process of alloy A. Symbols represents experimental data

Although there is a certain degree of dispersion of the points in several cases, the overall pattern is sufficiently good to justify the use of Eq. (1) to study the crystallization kinetics. In all processes, all graphs follow one master curve, the value of its JMAE kinetic exponent is not constant. Really, the n value changes continuously as a function of transformed fraction, to simplify the analysis we apply the least square sum, S, in several zones looking for the n value (with a 0.1 precision) that gives a best adjust. The S values ranged between 0.0128 and 0.0034. In the nearly stages, n changes steeply revealing the transient nucleation effect to reach the value ranging from 1.7 to 2.5 in the central part of the transformation ($0.3<x<0.55$). The 2.5 value corresponds to a three-dimensional volume growth controlled by diffusion. Latter in the transformation n continuously decreases ranging from 0.5 to 1.2. One possible

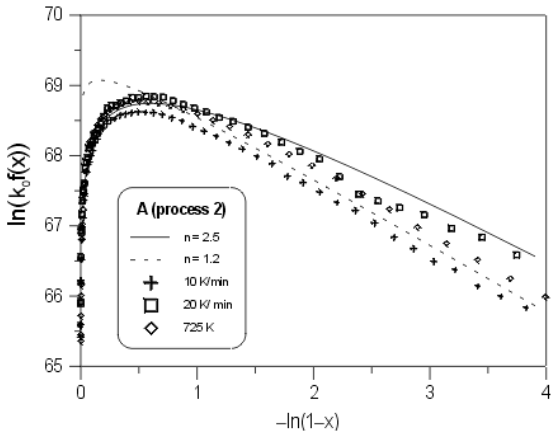

Fig. 2 Plot of $\ln(k_0 f(x))$ *vs*. $-\ln(1-x)$ for the high temperature crystallization process of alloy A. Symbols represents experimental data

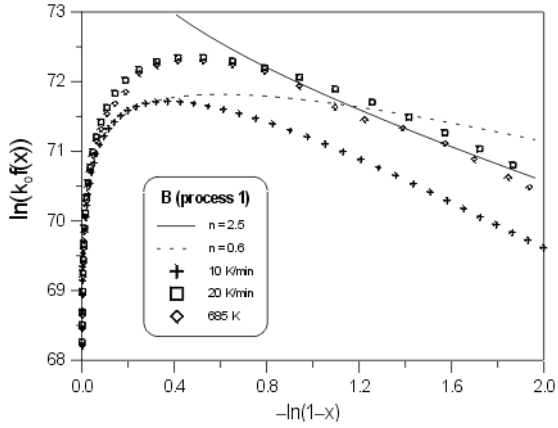

Fig. 3 Plot of $\ln(k_0 f(x))$ *vs*. $-\ln(1-x)$ for the low temperature crystallization process of alloy B. Symbols represents experimental data

cause is the influence of a second crystallization step, as detected in FeSiB glassy ribbons [20], but in our case both crystallization process are clearly differentiated. The most probable is that the n decrease reflects the saturation of nucleation [21]. Moreover, this complicated behavior is not surprising since not only nucleation and crystal growth but also change of composition of the crystalline phase can occur.

Furthermore, from the comparison of the activation energies values as shown at Table 1 and the maximum $\ln(k_0 f(x))$ value as determined in Figs 1 to 4 we can establish that a higher value on the crystallization activation energy corresponds to a higher value in the $\ln(k_0)$ (ranging between 107.3 and 56.7), this effect can be related

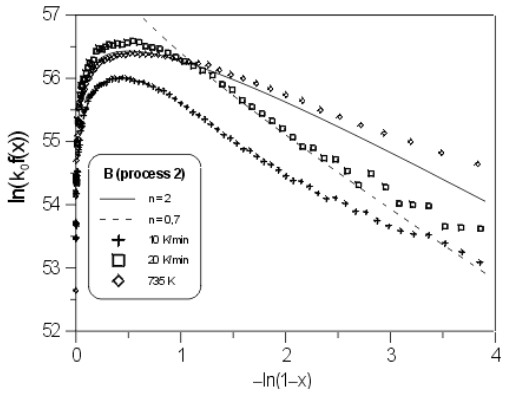

Fig. 4 Plot of $\ln(k_0 f(x))$ *vs*. $-\ln(1-x)$ for the high temperature crystallization process of alloy B. Symbols represents experimental data

to an apparent compensation effect [22] indicating a similar behavior of the crystalline phases.

Conclusions

Two Fe–Ni based quaternary glassy alloys were obtained by melt spinning: $Fe_{40}Ni_{40}P_{20-x}Si_x$ with x=7 and 10. The alloys presents two stages of crystallization well separated in temperature. The apparent activation energies, E, are obtained from Kissinger, Ozawa and multiple scan methods and ranging from 6.6 to 4.2 eV.

Although there is a certain degree of dispersion, the kinetic model that gives the best fit of the experimental data in the two stages of crystallization of both alloys is the Johnson–Mehl–Avrami–Erofeev (JMAE) equation. No significant changes are detected as a function of P/Si content. In all processes, all graphs follow one master curve. Moreover, the value of its JMAE kinetic exponent is not constant. In the nearly stages, n changes steeply revealing the transient nucleation effect to reach in the central part a value corresponding to growth controlled by diffusion. Latter in the transformation n continuously decreases reflecting the saturation of nucleation. Furthermore, an apparent compensation effect appears between activation energy and $\ln(k_0)$. To draw more valuable scientific conclusions it is necessary to extent the analysis to more compositions.

* * *

The work has been financed by MICYT grant MAT2000-0388 and Generalitat de Catalunya grant 1999SGR-0036.

References

1 G. Falkenhagen and W. Hoffman, Z. Metallk., (1952) 69.
2 P. Duwez, R. H. Willens and W. Klement, J. Appl. Phys., (1960) 1136.

3 P. Duwez, W. Klement and R. H. Willens, Nature, 186 (1960) 869.
4 Y. Yoshizawa, S. Oguma and K. Yamaguchi, J. Appl. Phys., 64 (1988) 6047.
5 E. Illekova, I. Mat'ko, P. Duhaj and F. A. Kuhnast, J. Mater. Sci., 32 (1997) 4645.
6 J. J. Suñol, N. Clavaguera and M. T. Mora, J. Therm. Anal. Cal., 52 (1998) 853.
7 T. Triwikantoro, D. Toma, M. Meuris and U. Koster, J. Non-Cryst. Solids, 252 (1999) 719.
8 B. X. Liu, W. S. Lai and Z. J. Zhang, Advances in Physics, 50 (2001) 367.
9 I. Virág, L. Pöppl and G. Várhegyi, Thermochim. Acta, 351 (2000) 79.
10 F. Branda, G. Luciani and A. Constantini, J. Therm. Anal. Cal., 61 (2000) 889.
11 J. J. Suñol, M. T. Clavaguera-Mora, N. Clavaguera and T. Pradell, Mater. Res. Soc. Symp. Proc., 455 (1997) 489.
12 T. Pradell, J. J. Suñol, N. Clavaguera and M. T. Clavaguera-Mora, J. Non-Cryst. Solids, 276 (2000) 113.
13 H. E. Kissinger, Anal. Chem., 29 (1957) 1702.
14 T. Ozawa, Bull. Chem. Soc. Japan., 38 (1965) 1881.
15 B. Carroll, Thermochim. Acta, 3 (1972) 449.
16 S. Bordas, M. T. Clavaguera-Mora and N. Clavaguera, J. Non-Cryst. Solids, 119 (1990) 232.
17 E. Illekova, Thermochim. Acta, 180/281 (1996) 289.
18 S. Suriñach, M. D. Baró, J. A. Diego, M. T. Clavaguera-Mora and N. Clavaguera, Acta Metall. Mater., 40 (1992) 37.
19 I. Mat´ko, E. Illekova, P. Svec, P. Duhaj and K. Czomorova, Mater. Sci. Eng. A, 226-228 (1997) 280.
20 I. Mat'ko, E. Illekova, P. Svec and P. Duhaj, Mater. Sci. Eng. A, 225 (1997) 145.
21 M. T. Clavaguera-Mora, S. Suriñach, M. D. Baró and N. Clavaguera, J. Mater. Sci., 18 (1983) 1381.
22 A. K. Galwey, Adv. Catal., 26 (1977) 247.